Bull. Mater. Sci., Vol. 36, No. 6, November 2013, pp. 1115–1119. © Indian Academy of Sciences.

Evidence for high ionic conductivity in lithium–lanthanum titanate, $Li_{0.29}La_{0.57}TiO_3$

D TIRUPATHI SWAMY[1,*], **K EPHRAIM BABU**[2] **and V VEERAIAH**[2]
[1]Department of Physics, Gitam Institute of Technology, Gitam University, Visakhapatnam 530 045, India
[2]Department of Physics, Andhra University, Visakhapatnam 530 003, India

MS received 14 March 2012; revised 5 August 2012

Abstract. Lithium–lanthanum titanate, $Li_{0.29}La_{0.57}TiO_3$, is prepared by solid-state reaction method and it is furnace-cooled to room temperature. X-ray diffraction results indicated that the compound has tetragonal perovskite-like structure and the lattice parameters are determined as $a = 3{\cdot}8714$ Å and $c = 7{\cdot}7370$ Å. The average grain size is found to be 5 μm from SEM micrograph. The analysis of FTIR and Raman spectra of the sample supported tetragonal structure inferred from XRD data. The impedance spectrum of the sample is separated into bulk and grain boundary parts by analysing the impedance data. The high bulk ionic conductivity is reported as $1{\cdot}12 \times 10^{-3}$ S cm^{-1} at room temperature. D.C. conductivity measurements indicate that the compound is a good ionic conductor.

Keywords. Perovskite; ionic conductivity; electrolyte.

1. Introduction

Among various rechargeable batteries, lithium-ion rechargeable batteries are extensively used in different applications because of their high energy density, better charge efficiency and wide electrochemical window, etc. But the liquid or organic polymer electrolytes used in lithium-ion batteries would cause safety problems. It is realized that the replacement of the liquid or organic electrolytes by inorganic solid-state electrolytes would be an efficient approach to solve their safety problems. The high ionic conductivity and good electrochemical stability are prerequisites for solid electrolytes. Lithium conducting oxides would meet these requirements. Hence, research on lithium–lanthanum titanates $Li_{3x}La_{2/3-3x}\square_{1/3-2x}TiO_3$ (where $\square$ = vacancy) has gained prominence during the last few years because of their high ionic conductivity at room temperature (about 10^{-3} S cm^{-1}). They possess perovskite-like structure. In perovskite-like structure, some of the La sites are occupied by vacancies. Hence, one La^{3+} ion can be easily substituted by three Li^+ ions. The migration of lithium-ion occurs through the bottleneck (shown in figure 1) formed by four TiO_6 octahedra.

It has been suggested that the high ionic conductivity is related to the size of the bottle-neck, the distribution of La^{3+} ions as obstacles against Li^+ ion migration and the number of defects at the Li sites. Recent investigations have been shown that tilting of TiO_6 octahedra changes the bottle-neck size, which is directly related to the Li^+ conductivity (Latie *et al* 1984; Inaguma *et al* 1993, 2002; Fourquet *et al* 1996; Belous 2001; Bohnke *et al* 2002).

It was also observed that there is a difference in ionic conductivity between furnace-cooled and quenched samples. The furnace-cooled sample has higher degree of order and the quenched sample has lower degree of order. At 300 K, the furnace-cooled sample has ionic conductivity higher than that of quenched sample (Inaguma *et al* 1997; Harada *et al*

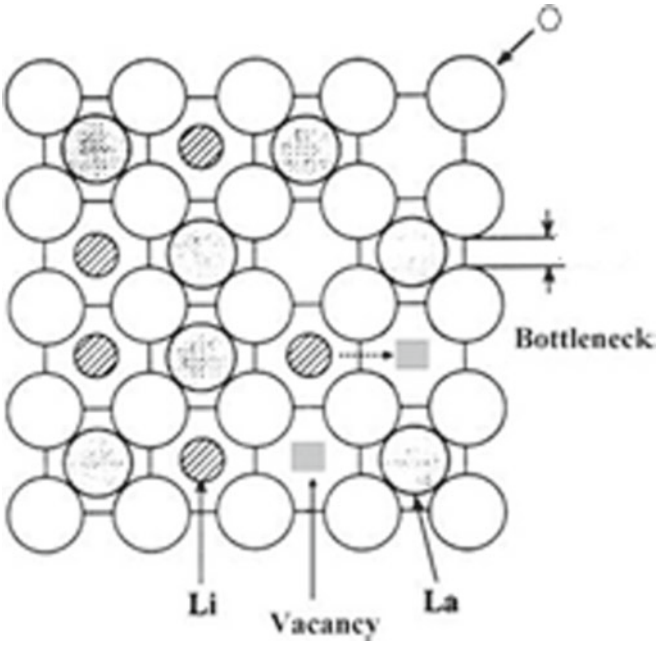

Figure 1. Schematic representation of bottleneck for lithium-ion conduction in perovskite-like structure (LLTO).

*Author for correspondence (swamydts@yahoo.co.in)

1998). It has been reported that the bulk conductivity was found to be closely related to the calcination temperature of the samples (Chen and Amine 2001).

In this paper, we report high ionic conductivity of the sample $Li_{0.29}La_{0.57}TiO_3$. The sample is prepared by solid-state reaction method, calcined at 1100 °C and is furnace cooled in view of achieving high ionic conductivity.

2. Experimental

The sample was synthesized by a conventional solid-state reaction method. The reaction equation is given below:

$$(0{\cdot}145)Li_2CO_3 + (0{\cdot}285)La_2O_3 + TiO_2 \rightarrow Li_{0.29}La_{0.57}TiO_3 + (0{\cdot}145)CO_2.$$

The starting materials were Li_2CO_3 (purity 99%, Sigma Aldrich), La_2O_3 (purity > 99·9%, Sigma Aldrich) and TiO_2 (purity 99·8%, Sigma Aldrich) taken in stoichiometric amounts. These were mixed thoroughly in an agate mortar and ground for 6 h. The mixture of starting materials was calcined at 850 °C for 4 h and then at 1100 °C for 12 h in air, in steps of 5 °C per min with intermediate grindings and then cooled to room temperature. The calcined powder was ground and pelletized after mixing poly vinyl alcohol (PVA) using hydraulic press at about 4 tonnes per cm^2. The size of the pellet was 12 mm in diameter and thickness was 1–2 mm. These pellets were sintered at 1300 °C for 6 h in air and cooled in the furnace. The powder XRD data of the samples were recorded on a PANalytic X'pert–PRO diffractometer using CuKα radiation and the microscopic studies were made using JEOL, JSM-6610 high resolution scanning electron microscope. FTIR spectra were recorded in KBr pellets using JASCO FTIR-5300 spectrometer. Raman spectra were recorded using thermo-nicolet 6700 FT–Raman spectrometer. Electrochemical impedance spectra were obtained in the frequency range of 1 Hz–6 MHz using Newton N4L, PSM 1735 impedance analyser. D.C. conductivity was measured using Aplab limited MT4090 LCR/ESR meter.

3. Results and discussion

XRD pattern of powder sample is shown in figure 2 from 20 to 80°. The diffraction pattern is analysed and indexed by X'pert-PRO high score plus software. All the peaks of $Li_{0.29}La_{0.57}TiO_3$ compare well with those reported in the literature (JCPDS). The crystal structure corresponds to *P*4/*mmm* space group. The powder X-ray diffraction pattern reveals a tetragonal system with perovskite-like structure. When LLTO is prepared by the conventional solid-state reaction followed by slow cooling to room temperature, XRD pattern shows superstructure lines (Fourquet *et al* 1996). The high temperature synthesis (1100–1300 °C) leads to a complete disordering of La^{3+} ions in the structure by thermal diffusion of La^{3+}. A slow cooling to room temperature favours some ordering of La^{3+} ions in *A*-cages of the

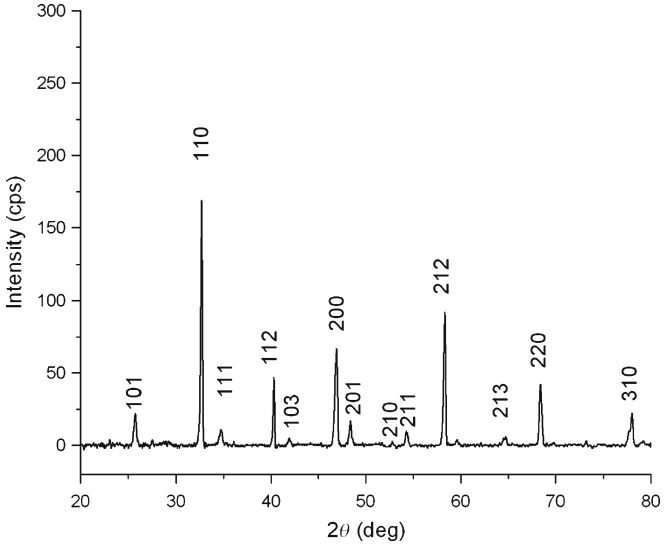

Figure 2. XRD pattern of $Li_{0.29}La_{0.57}TiO_3$.

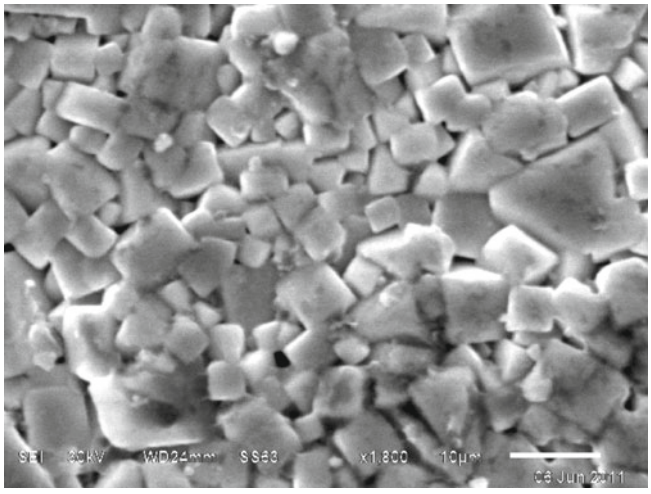

Figure 3. SEM micrograph of $Li_{0.29}La_{0.57}TiO_3$.

perovskite structure. LLTO is then structurally well described in *p*4/*mmm* space group (Fourquet *et al* 1996). In this structural model, La^{3+} ions are unequally distributed in the two adjacent *A*-cages of the perovskite network along *c* direction. This unequal distribution of La^{3+} ions is responsible for the doubling of the *c* axis parameter and for presence of the superstructure lines. This implies the existence of La^{3+}-rich layers and La^{3+}-poor layers in the perovskite structure. The lattice parameters are calculated and found to be $a = 3{\cdot}8714$ Å and $c = 7{\cdot}7370$ Å. The volume of the unit cell is 115·961 $(Å)^3$. The bulk density of the sintered pellet is determined by Archimedes principle and relative density of the sample is found to be more than 95%. The crystallite size is calculated using Scherrer's formula

$$\text{Crystallite size, } L = \frac{k\lambda}{\beta \cos\theta},$$

and is found to be 0·087 μm.

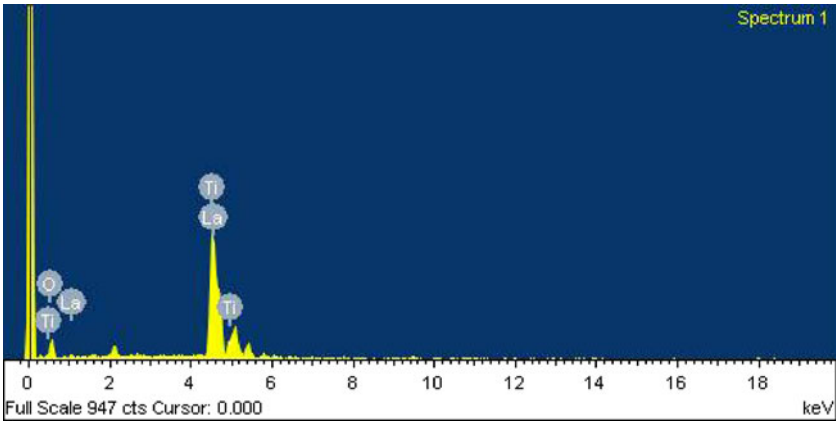

Figure 4. Energy dispersive spectrum of $Li_{0.29}La_{0.57}TiO_3$.

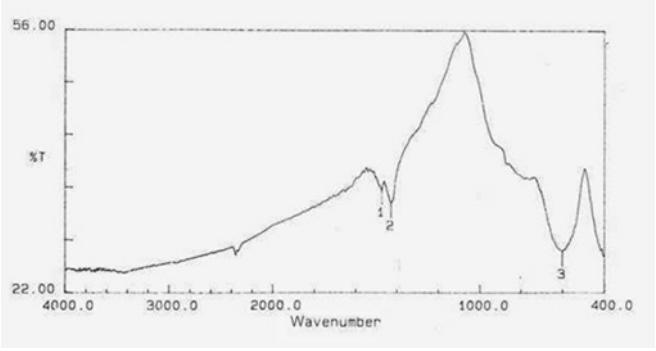

Figure 5. FTIR spectrum of $Li_{0.29}La_{0.57}TiO_3$.

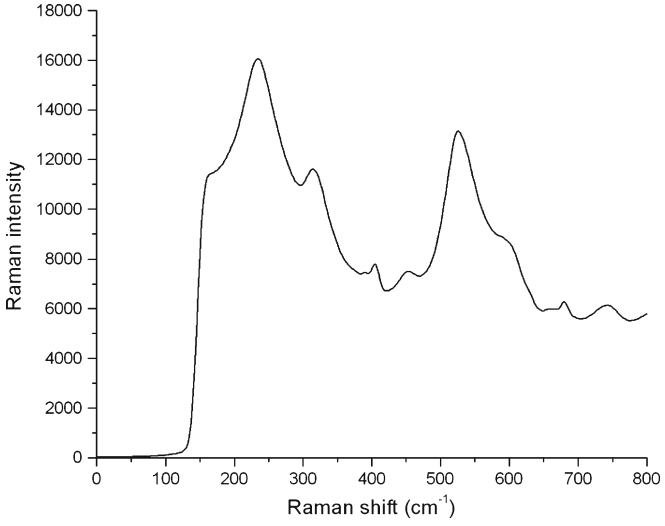

Figure 6. Raman spectrum of $Li_{0.29}La_{0.57}TiO_3$.

Surface morphology and grain size of the synthesized sample, $Li_{0.29}La_{0.57}TiO_3$, are observed by high resolution scanning electron microscopy (SEM). SEM micrograph of the sample is shown in figure 3. It reveals good compactness of grains and densification of the sample. The average grain size is found to be 5 μm by linear intercept method from SEM micrograph. The ceramic grains are in rectangular shape, characteristic of crystal lattice with lower than cubic symmetry (Fortal'nova *et al* 2006). The rectangular cross-section of the grains is in-line with the tetragonal cell symmetry observed from XRD data. Energy dispersive spectrum (EDS) of the sample is shown in figure 4. The analysis of the spectrum shows elements in the compound. SEM could not detect lighter elements like lithium and sodium. EDS reveals the presence of lanthanum, titanium and oxygen which are observed in the compound.

FTIR spectrum of the synthesized sample is recorded on KBr pellets. FTIR spectrum of $Li_{0.29}La_{0.57}TiO_3$ powder is presented in figure 5. FTIR spectrum of the sample indicates that the synthesized material has a distorted perovskite structure (Sych *et al* 1974). The absorption bands are identified at 601, 1429 and 1475 cm^{-1}. The band observed at 601 cm^{-1} is assigned to Ti–O stretching vibrations (Fortal'nova *et al* 2006). The observed bands at 1429 and 1475 cm^{-1} are assigned to Ti–O bending vibrations (Blanco Lopez *et al* 1999). Raman spectrum of $Li_{0.29}La_{0.57}TiO_3$ is presented in figure 6. Five to seven bands may be observed in the measured wavenumber range of Raman spectrum. The bands identified are 233, 315, 405, 453, 526, 679 and 743 cm^{-1}. The number of modes is in agreement with the prediction for a tetragonal (*p*4/*mmm*) perovskite cell (Varez *et al* 2001; Laguna *et al* 2002; Sanjuan *et al* 2005).

Li-ion conductivities are calculated by analysing the impedance data. The activation energy of the sample is calculated by measuring the conductivities over the temperature range from 300 to 473 K. In interpreting the impedance data for $Li_{0.29}La_{0.57}TiO_3$ solid electrolyte, an equivalent circuit proposed by Inaguma *et al* (1993) is used. The grain and grain boundary conductivities are determined using the following relations:

$$\sigma_{\text{bulk}} = \frac{L}{R_{\text{bulk}} A}\ \text{S cm}^{-1} \qquad \text{and} \qquad \sigma_{\text{gb}} = \frac{L}{R_{\text{gb}} A}\ \text{S cm}^{-1},$$

where L is the electrode separation (cm), A the electrode area (cm^2), R_{bulk} the bulk resistance of the sample and R_{gb} the grain boundary resistance of the sample.

The impedance spectrum can be divided into two parts, bulk crystal and grain boundary (Inaguma *et al* 1993). The semicircle with lower resistivity is observed which corresponds to bulk crystal part and another with higher resistivity corresponds to grain boundary part. The complex impedance plots of bulk (or grain part) and grain boundary parts of the sample at room temperature are presented in figure 7. The bulk conductivity and grain boundary conductivities are found to be $\sigma_g = 1{\cdot}12 \times 10^{-3}$ S cm^{-1} and $\sigma_{gb} = 2{\cdot}12 \times 10^{-5}$ S cm^{-1} at 300 K. The observed bulk conductivity is slightly higher than the value (1×10^{-3} S cm^{-1}) reported by Inaguma *et al* (1993). The factors like available space for Li^+ ion migration, the bottle-neck size formed by TiO_6 octahedra and vacancy concentration on A-site effect the ionic conduction in this perovskite type structure (Inaguma *et al* 1993; Oguni *et al* 1994; Thangadurai *et al* 1999; Jena *et al* 2005). In general, ionic conduction in these materials occurs due to the mobile ions hopping among energetically favourable sites. The motion of the surrounding ions simply provides the activation energy required for mobile ions to move through channels in the crystalline frame work (Park *et al* 2010). Thus, mobility mainly depends on the activation energy of the ionic conduction and the bottle-neck size of Li^+ ion conducting channel. The prepared LLTO has a number of vacancies on A-site which can be calculated from the relation, A-site vacancy = 1 – La content – Li content (Inaguma *et al* 1994). The considerable larger volume of the unit cell is reported in this paper. Thus, high ionic conductivity may be originated from the migration of Li^+ ions via vacancies on A-sites and through the wide bottle-neck size.

Arrhenius plot of bulk conductivity of the sample is shown in figure 8, which is almost linear. Arrhenius behaviour indicates the temperature dependence of ionic conductivity of the sample. The activation energy of the sample is calculated from the slope of Arrhenius plot obtained by taking log σ on y-axis and 1000/T on x-axis. The activation energy of the bulk conduction is found to be 0·19 eV which agrees well with the reports of Inaguma *et al* (1993) and Chen and Amine (2001).

The variation of real and imaginary parts of impedance with frequency in the temperature range 300–473 K is shown in figure 9. The magnitude of Z' decreases with temperature which indicates increase in a.c. conductivity. Z' values merge at high frequencies at all temperatures. The real part of impedance merges at higher frequencies for all the temperatures indicating release of space charges. Z'' values shift to lower frequencies with decreasing temperature indicating decreasing relaxation in the system (Srinivas *et al* 2003). D.C. conductivity is measured in the temperature range 300–473 K. D.C. conductivity is observed as $1{\cdot}9 \times 10^{-8}$ S cm^{-1} at

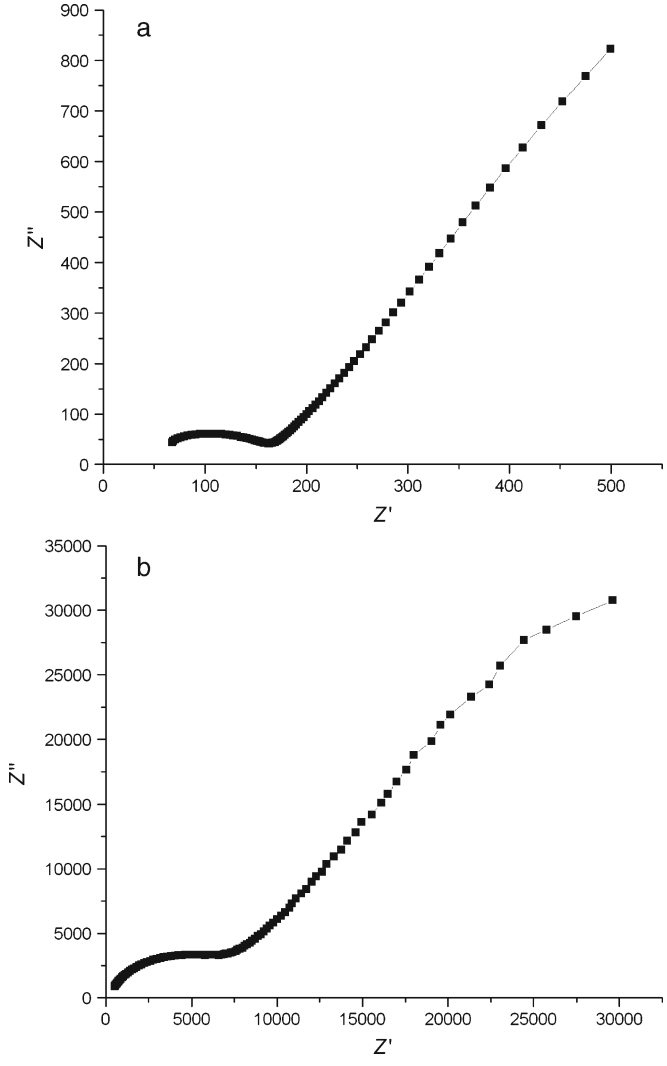

Figure 7. Complex impedance plot for (**a**) bulk conductivity and (**b**) grain boundary conductivity of $Li_{0.29}La_{0.57}TiO_3$.

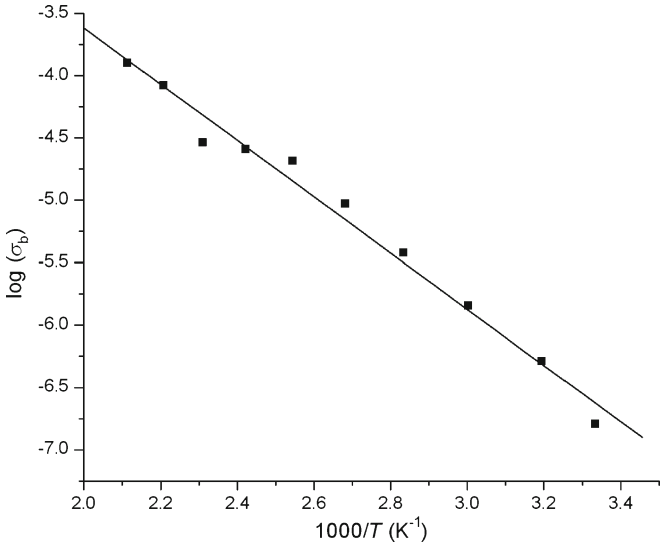

Figure 8. Arrhenius plot of bulk conductivity of $Li_{0.29}La_{0.57}TiO_3$.

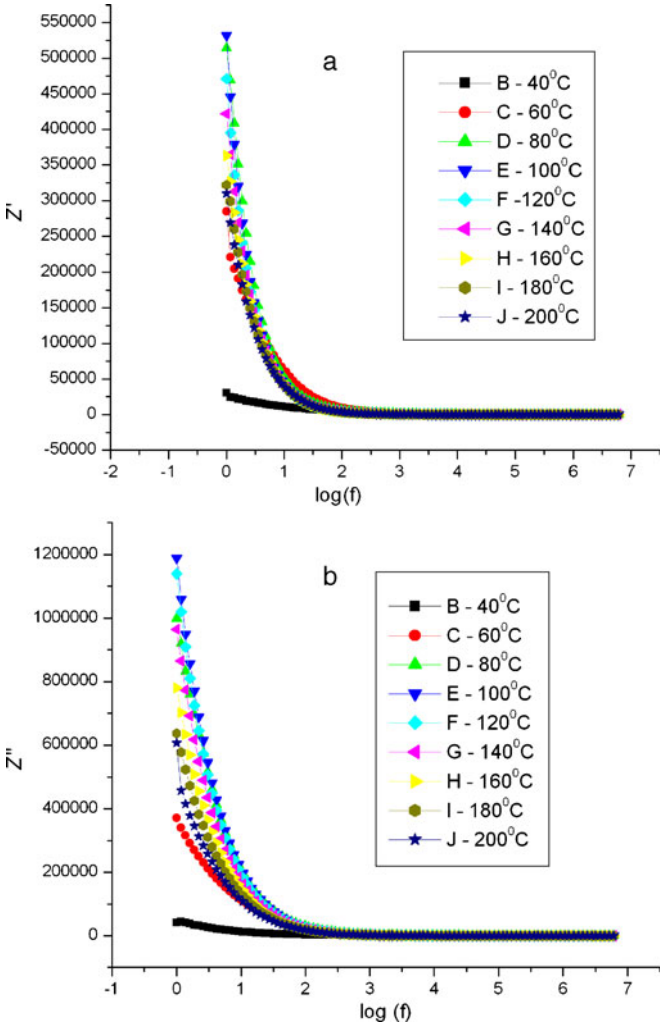

Figure 9. Variations of (**a**) real part of impedance (Z′) and (**b**) imaginary part of impedance (Z″) of $Li_{0.29}La_{0.57}TiO_3$.

room temperature. These results are in good agreement with reported values of electronic conduction values in the range 5×10^{-9}–1×10^{-8} S cm^{-1} at room temperature (Stramare *et al* 2003).

4. Conclusions

The crystal has tetragonal perovskite type structure with space group, *p*4/*mmm* (123). FTIR spectrum of sample indicated that the synthesized solid solution has a distorted perovskite structure. From Raman spectrum, the number of modes observed is in good agreement with the prediction for a tetragonal (*p*4/*mmm*) perovskite cell. The observed bulk conductivity is higher than the reported value. The activation energy is estimated to be 0·19 eV for the bulk conduction. D.C. conductivity measurements showed that the observed value of conductivity is $1{\cdot}9 \times 10^{-8}$ S cm^{-1} at room temperature which is in the order of electronic conduction and hence, it is an evidence for the ionic conduction in the sample. Therefore, the sample is a good ionic conductor at low temperatures as well as at high temperatures and a good candidate as an electrolyte for electrochemical cells.

Acknowledgements

We thank Gitam University, Visakhapatnam, India, for providing financial assistance for this work.

References

Belous A G 2001 *J. Eur. Ceram. Soc.* **21** 1797
Blanco Lopez M C, Foularis G, Rand B and Railey F L 1999 *J. Am. Ceram. Soc.* **82** 1777
Bohnke O, Duroy H, Fourquet J L, Ronchetti S and Mazza D 2002 *Solid State Ionics* **149** 217
Chen C H and Amine K 2001 *Solid State Ionics* **144** 51
Fortal'nova E A, Mosunov A V, Safraonenko M G, Venkovskii N U and Politova E D 2006 *Inorg. Mater.* **42** 393
Fourquet J L, Duroy H and Crosnier-Lopez M P 1996 *J. Solid State Chem.* **127** 283
Harada Y, Ishigaki T, Kawai H and Kuwano J 1998 *Solid State Ionics* **108** 407
Inaguma Y, Liquan C, Itoh M, Nakamura T, Uchida T, Ikuta H and Wakihara M 1993 *Solid State Commun.* **86** 689
Inaguma Y, Katsumata T, Yu J and Itoh M 1997 *Mater. Res. Soc. Symp. Proc.* **453** 623
Inaguma Y, Katsumata T, Itoh M and Morii Y 2002 *J. Solid State Chem.* **166** 67
Inaguma Y, Chen L, Itoh M and Nakamura T 1994 *Solid State Ionics* **70/71** 196
Jena Hrudananda, Govindan Kutty K V and Kutty T R N 2005 *J. Mater. Sci.* **40** 4737
Laguna M A, Sanjuan M L, Varez A and Sanz J 2002 *Phys. Rev. B* **66** 54301
Latie L, Villeneuve G, Conte D and Le Flem G 1984 *J. Solid State Chem.* **51** 293
Oguni M, Inaguma Y, Itoh M and Nakamura T 1994 *Solid State Commun.* **91** 627
Park M, Zhang X, Chung M, Less G B and Sastry A M 2010 *J. Power Sources* **195** 7904
Sanjuan M L, Laguna M A, Belous A G and V'yunov O I 2005 *Chem. Mater.* **17** 5862
Srinivas K, Sarah P and Suryanarayana S V 2003 *Bull. Mater. Sci.* **26** 247
Stramare S, Thangadurai V and Weppner W 2003 *Chem. Mater.* **15** 3974
Sych A M, Klenus V G and Demyanenko V P 1974 *Ukr. Fiz. Zh.* **19** 505
Thangadurai V, Shukla A K and Gopalakrishnan J 1999 *Chem. Mater.* **11** 835
Varez A, Sanjuan M L, Laguna M A, Penna J I, Sanz J and de la Fuente G F 2001 *J. Mater. Chem.* **11** 125